JOURNAL OF AGRICULTURAL AND FOOD CHEMISTRY

FT-IR Investigation of Cell Wall Polysaccharides from Cereal Grains. Arabinoxylan Infrared Assignment

PAUL ROBERT,† MÉLANIE MARQUIS,† CÉCILE BARRON,§ FABIENNE GUILLON,† AND LUC SAULNIER*,†

INRA—Unité de Recherches Biopolymères, Interactions et Assemblages, B.P. 71627, 44316 Nantes Cedex, France, and Unité mixte de Recherches Ingénierie des Agropolymères et Technologies Emergentes, INRA-ENSAM-UMII-CIRAD, 2 place Viala, 34060 Montpellier Cedex 1, France

The FT-IR fingerprint of wheat endosperm arabinoxylan (AX) was investigated using a set of polysaccharides exhibiting variation of their degree of substitution and xylo-oligosaccharides comprising xylose units mono- or disubstituted by arabinose residues. Substitution of the xylose backbone by arabinose side units was more particularly studied in the 1000−800 cm^{-1} spectral region, by taking advantage of second-derivative enhancement. The 920−1020 cm^{-1} spectral region revealed two absorption bands at 984 and 958 cm^{-1}, the intensities of which varied according to the degree of substitution. Whereas the intensity of the band at 958 cm^{-1} increased with the degree of substitution, that at 984 cm^{-1} decreased. The second-derivative spectral data of xylo-oligosaccharides indicated that these changes could be attributed to substitution of the xylan backbone by arabinose residues, and the band at 958 cm^{-1} was ascribed to the presence of disubstituted xylose residues. Principal component analysis of FT-IR spectra of model mixtures of AX, β-glucans, and arabinogalactans suggested that it is possible to evaluate the relative proportions of the polymers and degree of substitution of AX in complex mixtures such as the cell wall of cereal grains.

KEYWORDS: Hemicellulose; β-glucan; arabinogalactan; pentosan; wheat; principal component analysis

INTRODUCTION

Arabinoxylans (AX) are the predominant nonstarch polysaccharides from cereal grain cell walls of endosperm. They are involved in many cereal uses such as breadmaking, poultry feeding, or brewing (*1*, *2*). AX are closely associated with mixed linked β-(1−3, 1−4)-glucans (BG) in endosperm cell walls of cereal grains (*1*). BG in wheat endosperm represent ∼20% of the cell wall, but they can account for up to 70% of the cell walls in barley or oat. AX consist in a linear backbone of β-(1→4) linked D-xylopyranosyl units, which are unsubstituted (uXyl), monosubstituted (mXyl) on O-3, or disubstituted (dXyl) on O-3 and O-2 with α-L-arabinofuranosyl units. In wheat endosperm ∼25% of AX are water extractable (WE-AX). Besides WE-AX, arabinogalactans (AG) are water-soluble polymers that are coextracted when flour or grain is submitted to water extraction. Whereas AG extracted from 100 g of wheat flour may represent 0.3−0.4 g (*3*, *4*), WE-AX ranges from 0.3 to 1 g (*5*).

WE-AX exhibit large natural variations in their structure, which are depicted by their relative proportion of uXyl (60−65%), mXyl (12−20%), and dXyl (15−30%) (*6*−*9*). Structural changes are also expressed in terms of arabinose to xylose molar ratio (A/X) with typical average values of 0.5−0.6. Extreme A/X values ranging from 0.31 to 1.06 were reported for WE-AX subfractions isolated by ethanol precipitation and gel permeation chromatography (*10*, *11*). However, the major part of AX in endosperm cell walls of wheat grains are water unextractable (WU-AX) and have been studied after alkaline extraction (*12*−*15*) or enzymatic solubilization (*5*). Their structures exhibit variations (*5*) and basically correspond to that of WE-AX with a slightly higher A/X ratio due to a higher proportion of monosubstituted residues.

The substitution pattern of AX is easily distinguishable by proton NMR spectroscopy (*16*, *17*). However, NMR requires relatively high amounts of material and has been mainly applied to isolated fractions, which limits its use in many respects. Infrared spectroscopy presents the advantage of being rapid and sensitive. In addition, due to various sampling techniques, vibrational spectroscopy makes it possible to study a wide range of carbohydrates in different physical states. Infrared spectroscopy has been proved to be useful for studying physicochemical and conformational properties of carbohydrates (*18*, *19*). Infrared (micro)spectroscopy has recently been applied to the study of plant cell wall architecture despite the complexity of the system (*20*) and to the screening of cell wall mutants of *Arabidopsis* (*21*, *22*).

* Author to whom correspondence should be addressed (e-mail saulnier@nantes.inra.fr).
† INRA—Unité de Recherches Biopolymères.
§ Unité mixte de Recherches Ingénierie des Agropolymères et Technologies Emergentes.

10.1021/jf051145y CCC: $30.25
Published on Web 08/09/2005

Although a precise assignment of polysaccharide spectra remains difficult, each particular polysaccharide has a specific band maximum in the 1200−800 cm^{-1} region (*23*). For example, the high homogalacturonan content in pectin samples gives rise to characteristic absorption bands at 1100 and 1017 cm^{-1}, and the linear and branched (1→4)-β-xylans reveal a band maximum at about 1047 cm^{-1}. In arabinogalactans, two strong bands observed at about 1075 and 1045 cm^{-1} characterize galactopyranose in the backbone and arabinofuranose units in side branches, respectively. (1→4)-β-Glucans are identified by an absorption band at around 1030 cm^{-1}.

A detailed assignment of the xylan infrared spectrum was previously investigated (*24*). The acid or salt state of glucuronic acid side chains can be recognized by the presence of a band at either 1725 or 1600 cm^{-1}. A strong absorption band at 1250 cm^{-1} characterizes *O*-acetyl samples. As in native cellulose, the band at 1160 cm^{-1} was assigned to the antisymmetric C−O−C stretching mode of the glycosidic link and that at about 895 cm^{-1} to the β configuration of C_1. The shape of xylan infrared spectra strongly depends on the degree of substitution and on the presence of arabinose or glucuronic units on O-2 or O-3 (*25*, *26*). In the case of arabinoxylan highly substituted with arabinose on O-3, the intensity of the band assigned to the glycosidic bond at about 1160 cm^{-1} decreases. The decrease at 1160 cm^{-1} is accompanied with a decrease of the absorption band at about 990 cm^{-1}. Arabinose or glucuronic substitution on O-2 does not significantly affect the infrared spectrum.

In the present paper, the infrared spectra of wheat endosperm AX was investigated using a set of polysaccharides isolated and characterized for their molecular weight and degree of substitution (*10*, *11*). In addition, the set of samples included xylo-oligosaccharides comprising xylose units mono- or disubstituted by arabinose (*27*, *28*). Substitution of the xylose backbone by arabinose side units was more particularly studied in the 1000−800 cm^{-1} spectral region, by taking advantage of second-derivative enhancement. The ability of infrared spectroscopy to evaluate the content and degree of substitution of AX was investigated in model mixtures containing AG or BG.

MATERIALS AND METHODS

Oligosaccharides and Polysaccharides. Water-extractable AX samples with different arabinose-to-xylose ratios (A/X, 0.37, 0.57, and 0.75) were subfractions isolated by size exclusion chromatography from graded ethanol fractionation (saturation level of ethanol, 30, 50, and 60%) of WE-AX (*10*). Mixed-linked β-(1−3, 1−4) glucans (BG, barley β-glucan, medium viscosity) was purchased from Megazyme (Bray, Ireland). Arabinogalactan protein (AG) was isolated from a graded ethanol fractionation of a water extract of wheat flour in 70% saturation fraction. The polymer contained mainly arabinose and galactose (35.4 and 47.8%, respectively; g/100 g) and minor amounts of xylose, glucose, and mannose (1.8, 1.7, and 0.9%, respectively).

Xylo-oligosaccharides substituted by arabinose were prepared from WE-AX by using an endoxylanase from *Trichoderma viride* (M1, Megazyme as previously described (*27*), whereas xylotetraose (X4) was purchased from Megazyme. Xylotetraoses monosubstituted by arabinose on position O-3 on the third xylose residue (A_1X_4) or disubstituted by arabinose on positions O-2 and O-3 on the third xylose residue (A_2X_4) were used (*28*).

Infrared Spectroscopy. FT-IR spectra were recorded in the transmission mode on thin films obtained by drying 0.5 mL of aqueous solutions (5 mg/mL) at 40 °C for 4 h. Model mixtures of polysaccharides were prepared by mixing an aqueous solution of AX (5 mg/mL) with a solution of BG (5 mg/mL) or AG (5 mg/mL) in a ratio fom 80:20 to 50:50 (v/v). Films were made by drying 0.5 mL of the mixture at 40 °C for 4 h. The infrared spectra were collected on a Vector 22 spectrometer (Bruker, France) equipped with a DTGS detector. They were recorded between 800 and 1200 cm^{-1} at 4 cm^{-1} resolution and resulted from the co-addition of 200 scans. The spectra were smoothed and their baselines corrected using the OPUS software. They were normalized as follows: (i) the average absorbance value was calculated and then subtracted to pull down to zero the middle of the spectrum; (ii) the sum of the squares of the resulting spectral data was calculated, and the spectrum was divided by the square root of the sum.

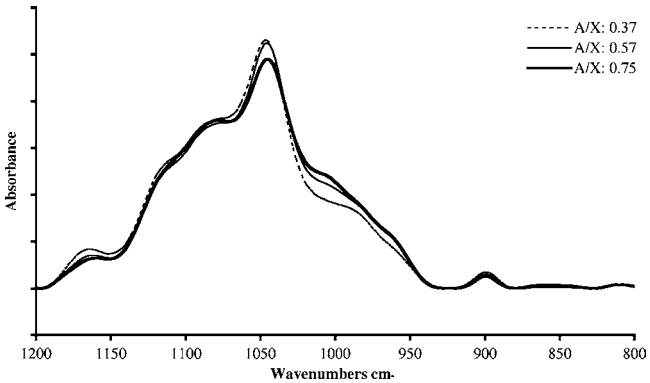

Figure 1. FT-IR spectra in the 1200–800 cm^{-1} region of AX presenting various degrees of substitution.

Data Treatments. Second-derivative spectral data were assessed to enhance spectral differences in the 1010−930 cm^{-1} region. The second-derivative data were obtained by using the Savitzky−Golay algorithm, developed on the OPUS-NT (Bruker) software.

Principal component analysis (PCA) was applied to the second-derivative spectral data. This multivariate data treatment made it possible to handle large data tables without making any preliminary assumption (*29*). The computation of principal components is based on the diagonalization of the variance−covariance matrix **V** assessed from the spectral data **X**. The diagonalization realizes a decomposition of **V** into eigenvectors **L** and eigenvalues **S**. The eigenvalues describe the amount of total variance taken into account by the principal components. The eigenvectors are used to assess the principal component scores **C**

$$\mathbf{V} = \mathbf{X}'\mathbf{X} \qquad \mathbf{C} = \mathbf{XL}$$

where **X** is the matrix of the spectral data (n samples × m wavenumbers) and **X′** is the transpose matrix of **X**.

The principal component scores are used to draw similarity maps that allow a comparison of the spectra to each other. Characteristic absorption bands are depicted using the spectral patterns derived from the eigenvectors.

RESULTS AND DISCUSSION

Infrared Spectra of Pure Arabinoxylan and Oligosaccharides. FT-IR spectra of AX presenting various degrees of substitution (A/X, 0.37, 0.57, and 0.75) are shown in **Figure 1**. The spectra are typical of polysaccharides in the 1200−800 cm^{-1} region with an absorption band assigned to glycosidic linkages at about 1160 cm^{-1} and a band characteristic of β-(1→4) linkages at 895 cm^{-1}. All AX spectra presented a maximum absorption band that might be assigned to C−OH bending around 1045 cm^{-1}. They were almost superimposed and showed only tiny differences in the 920−1020 cm^{-1} spectral region. A careful examination of the spectra between 920 and 1020 cm^{-1} was, therefore, carried out using second-derivative spectral data (**Figure 2**). The 920−1020 cm^{-1} spectral region revealed two absorption bands at 984 and 958 cm^{-1}, the intensities of which varied according to the degree of substitution. Whereas the intensity of the band at 958 cm^{-1} increased with the degree of substitution, that at 984 cm^{-1} decreased.

The proportion of mono- and disubtitution in AX is related to the A/X ratio, and it has been shown that disubstitution

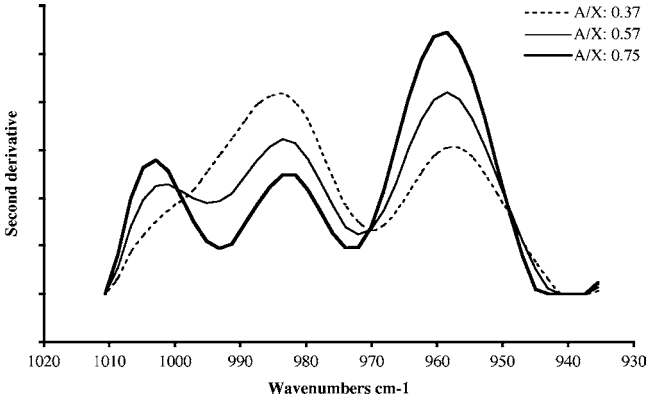

Figure 2. Second-derivative spectra of the 1010–935 cm^{-1} region for AX presenting various degrees of substitution. Second-derivative data are multiplied by –1.

Table 1. Proportion of Un- (uXyl), Mono- (mXyl), or Disubstituted (dXyl) Xylose Residues in AX of Different A/X Ratios As Determined by ^1H NMR

	A/X	uXyl	mXyl	dXyl
$AX_{0.37}$	0.37	71.7	19.5	8.7
$AX_{0.57}$	0.57	66.2	11.5	22.2
$AX_{0.75}$	0.75	58.4	10.0	31.5

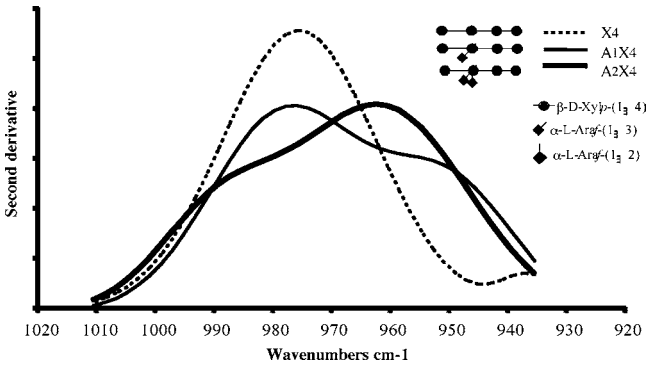

Figure 3. Second-derivative spectra of the 1010–935 cm^{-1} region for xylotetraose (X_4) and mono- (A_1X_4) and disubstituted (A_2X_4) oligomers. Second-derivative data are multiplied by –1.

increased with the A/X ratio. The relationship between disubstitution and A/X ratio has been confirmed by NMR study of the different fractions (**Table 1**). The second-derivative spectral data of xylo-oligosaccharides (**Figure 3**) indicated that changes in the 920−1020 cm^{-1} region could be attributed to substitution of the xylan backbone by arabinose residues. Whereas both xylotetraose and A_1X_4 had maximum absorption bands at 975 cm^{-1}, A_2X_4 exhibited a maximum at 960 cm^{-1}. Xylotetraose differed from A_1X_4 by the absence of a band at about 950 cm^{-1}.

This is the first time that IR was proved to be relevant for the characterization of fine structural features of AX. This spectral information can be useful to study AX in complex mixtures such as the cell wall of grains or grain water extract. To assess these possibilities we therefore run spectra on model mixtures.

Infrared Study of Model Mixtures Containing AX, BG, and AG. The infrared spectra of BG and AG, recorded in the 1200−800 cm^{-1} region, are shown **Figure 4**. BG exhibited an absorption band at 895 cm^{-1} assigned to $\beta(1-4)$ linkage. In addition, two broad and intense bands and a shoulder were

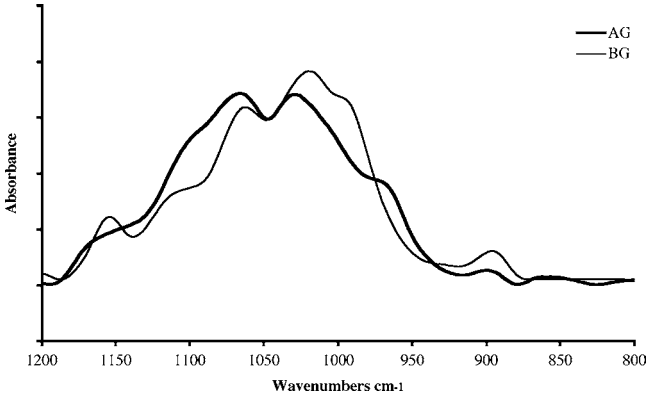

Figure 4. FT-IR spectra in the 1200–800 cm^{-1} region for β-glucans (BG) and arabinogalactan (AG).

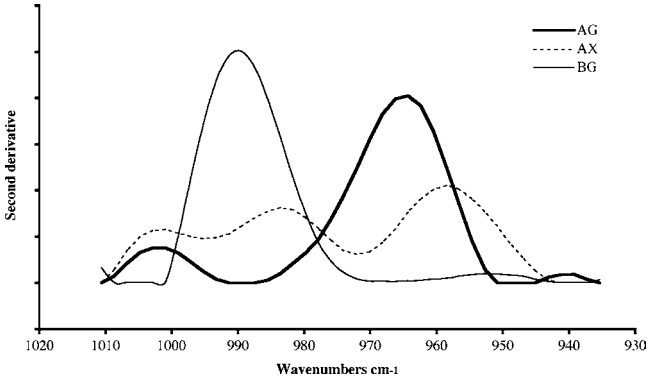

Figure 5. Second-derivative spectra of the 1010–935 cm^{-1} region for BG, AG, and AX. Second-derivative data are multiplied by –1.

observed at about 1065, 1020, and 990 cm^{-1}. AG also revealed two maxima around 1065 and 1020 cm^{-1} and a shoulder at 964 cm^{-1}.

A more detailed observation of the 1020−920 cm^{-1} spectral region of BG and AG was realized using second-derivative data. **Figure 5** compares the second-derivative spectra of BG and AG with that of AX. Whereas AX exhibited two bands at 982 and 956 cm^{-1}, AG and BG were characterized by only one absorption band at 964 and 991 cm^{-1}, respectively. The differences observed between AX, BG, and AG suggested that infrared spectroscopy might be very useful for studying AX in complex systems. A simultaneous determination of AX content and arabinose substitution could be considered.

As the absorption bands of AX, AG, and BG were very close together, they remained partially overlapping in mixtures. The second-derivative spectra of mixtures containing AX, AGp, and BG were, therefore, submitted to PCA. The first two principal components took 81 and 14% of the total inertia into account. The similarity map defined by principal components 1 and 2 separated the samples according to polymer proportions and A/X ratio (**Figure 6**). Mixtures enriched in AG were identified by negative scores along principal component 1, and samples enriched in BG were characterized by positive scores. In addition, a separation of the samples according to the A/X ratio was observed along the second principal component. A study of the loading plots associated with principal components 1 and 2 made it possible to explore the spectral features that discriminated the samples. The first spectral pattern (**Figure 7**) revealed an opposition between peaks at about 991 cm^{-1} (positive peak) and 964 cm^{-1} (negative peak). Whereas an absorption band at about 991 cm^{-1} was already observed for BG, a peak at 964 cm^{-1} was assigned to AG (**Figure 5**). The

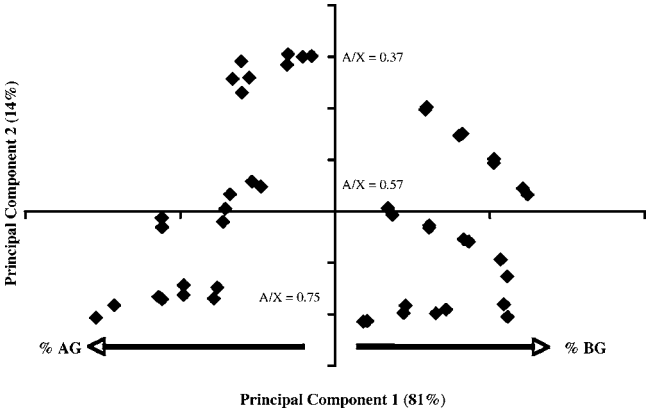

Figure 6. Similarity map from PCA of FT-IR spectra (second derivative of the 1010–935 cm^{-1} region) of mixtures containing AX of different degrees of substitution (A/X, 0.37, 0.54, and 0.75) and different relative proportions of AG or BG.

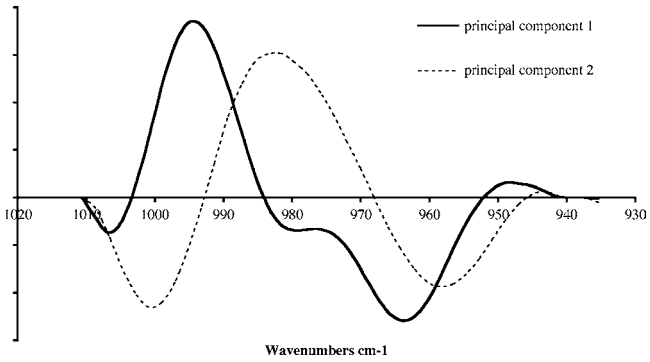

Figure 7. Spectral pattern obtained from PCA loadings, showing influent wavenumbers for the discrimination of polymer mixture.

discrimination of the samples according to A/X along principal component 2 resulted from an opposition between peaks at 984 and 958 cm^{-1}. The increase at 958 cm^{-1}, accompanied by a decrease at 984 cm^{-1} characterized the presence of highly substituted AX in mixtures.

Conclusion. This is the first time that IR was proved to be relevant for the characterization of fine structural features of AX. We have shown using model mixtures that AX, BG, and AG can be distinguished on the basis of their spectral behavior and that it was possible to estimate the relative proportions of the polymers as well as the fine structure of AX in complex mixtures. Using principal component regression, it is possible to envisage AX determination in grain water extracts. However, a particular study using a large data set will be necessary to get a robust equation of prediction. Furthermore, preliminary experiments indicated that quantification of AX in grain or flour water extracts requires the removal of starch in the samples. Starch presents infrared bands overlapping those of AX, BG, and AG in the 1200−800 cm^{-1} spectral region. In particular, the starch spectrum shows absorption bands at 1150, 1124, and 1103 cm^{1} (C−O and C−C stretching), 1077, 1047, 1022, 994, and 928 cm^{-1} (C−O−H bending, CH_2 modes), and 861 cm^{-1} (C−O−C stretching) (*30*−*32*).

Cell walls of the grain are complex mixture of polymers, mainly constituted by AX and BG in the endosperm. Previous studies using FTIR microspectroscopy have revealed microheterogeneity of arabinoxylans in endosperm cell walls (*33*, *34*). The information provided in the present paper will be useful to interpret the variation of spectral behavior of cell walls within grain tissues and will be further used to reveal spatial intensity and distribution of AX during grain development. Such information can also be used for plant breeding programs for selecting superior varieties of plants for targeted purposes and for prediction of food quality and nutritive value (*35*).

LITERATURE CITED

(1) Fincher, G. B.; Stone, B. A. Cell walls and their components in cereal grain technology. In *Advances in Cereal Science and Technology*; Pomeranz, Y., Ed.; American Association of Cereal Chemists: St. Paul, MN, 1986; pp 207−295.

(2) Courtin, C. M.; Delcour, J. A. Arabinoxylans and endoxylanases in wheat flour bread-making. *J. Cereal Sci.* **2002**, *35*, 225−243.

(3) Van den Bulck, K.; Swennen, K.; Loosveld, A.-M. A.; Courtin, C. M.; Brijs, K.; Proost, P.; Van Damme, J.; Van Campenhout, S.; Mort, A.; Delcour, J. A. Isolation of cereal arabinogalactan-peptides and structural comparison of their carbohydrate and peptide moieties. *J. Cereal Sci.* **2005**, *41*, 59−67.

(4) Loosveld, A. M. A.; Grobet, P. J.; Delcour, J. A. Contents and structural features of water-extractable arabinogalactan in wheat flour fractions. *J. Agric. Food Chem.* **1997**, *45*, 1998−2002.

(5) Ordaz-Ortiz, J. J.; Saulnier, L. Structural variability of arabinoxylans from wheat flours. Comparison of water-extractable and xylanase-extractable arabinoxylans. *J. Cereal Sci.* **2005**, *42*, 119−125.

(6) Cleemput, G.; Roels, S. P.; Vanoort, M.; Grobet, P. J.; Delcour, J. A. Heterogeneity in the Structure of Water-Soluble Arabinoxylans in European Wheat Flours of Variable Bread-Making Quality. *Cereal Chem.* **1993**, *70*, 324−329.

(7) Andersson, R.; Westerlund, E.; Aman, P. Natural Variations in the Contents of Structural Elements of Water-Extractable Nonstarch Polysaccharides in White Flour. *J. Cereal Sci.* **1994**, *19*, 77−82.

(8) Delcour, J. A.; Van Win, H.; Grobet, P. J. Distribution and structural variation of arabinoxylans in common wheat mill streams. *J. Agric. Food Chem.* **1999**, *47*, 271−275.

(9) Izydorczyk, M. S.; Biliaderis, C. G. Cereal arabinoxylans: advances in structure and physicochemical properties. *Carbohydr. Polym.* **1995**, *28*, 33−48.

(10) Dervilly, G.; Saulnier, L.; Roger, P.; Thibault, J. F. Isolation of homogeneous fractions from wheat water-soluble arabinoxylans. Influence of the structure on their macromolecular characteristics. *J. Agric. Food Chem.* **2000**, *48*, 270−278.

(11) Dervilly-Pinel, G.; Thibault, J. F.; Saulnier, L. Experimental evidence for a semi-flexible conformation for arabinoxylans. *Carbohydr. Res.* **2001**, *330*, 365−372.

(12) Gruppen, H.; Hamer, R. J.; Voragen, A. G. J. Water-Unextractable Cell-Wall Material from Wheat-Flour. 2. Fractionation of Alkali-Extracted Polymers and Comparison with Water-Extractable Arabinoxylans. *J. Cereal Sci.* **1992**, *16*, 53−67.

(13) Gruppen, H.; Hamer, R. J.; Voragen, A. G. J. Water-Unextractable Cell-Wall Material from Wheat-Flour. 1. Extraction of Polymers with Alkali. *J. Cereal Sci.* **1992**, *16*, 41−51.

(14) Gruppen, H.; Hamer, R. J.; Voragen, A. G. J. Barium Hydroxide as a Tool to Extract Pure Arabinoxylans from Water-Insoluble Cell-Wall Material of Wheat-Flour. *J. Cereal Sci.* **1991**, *13*, 275−290.

(15) Gruppen, H.; Kormelink, F. J. M.; Voragen, A. G. J. Water-unextractable Cell Wall Material from Wheat Flour. 3. A Structural Model for Arabinoxylans. *J. Cereal Sci.* **1993**, *18*, 111−128.

(16) Hoffmann, R. A.; Kamerling, J. P.; Vliegenthart, J. F. G. Structural Features of a Water-Soluble Arabinoxylan from the Endosperm of Wheat. *Carbohydr. Res.* **1992**, *226*, 303−311.

(17) Bengtsson, S.; Andersson, R.; Westerlund, E.; Aman, P. Content, Structure and Viscosity of Soluble Arabinoxylans in Rye Grain from Several Countries. *J. Sci. Food Agric.* **1992**, *58*, 331−337.

(18) Wilson, R. H.; Smith, A. C.; Kacurakova, M.; Saunders, P. K.; Wellner, N.; Waldron, K. W. The mechanical properties and molecular dynamics of plant cell wall polysaccharides studied by Fourier transform infrared spectroscopy. *Plant Physiol.* **2000**, *124*, 397−405.

(19) Kacurakova, M.; Wilson, R. H. Developments in mid-infrared FT-IR spectroscopy of selected carbohydrates. *Carbohydr. Polym.* **2001**, *44*, 291−303.
(20) McCann, M. C.; Bush, M.; Milioni, D.; Sado, P.; Stacey, N. J.; Catchpole, G.; Defernez, M.; Carpita, N. C.; Hofte, H.; Ulvskov, P.; Wilson, R. H.; Roberts, K. Approaches to understanding the functional architecture of the plant cell wall. *Phytochemistry* **2001**, *57*, 811−821.
(21) Chen, L. M.; Carpita, N. C.; Reiter, W. D.; Wilson, R. H.; Jeffries, C.; McCann, M. C. A rapid method to screen for cell-wall mutants using discriminant analysis of Fourier transform infrared spectra. *Plant J.* **1998**, *16*, 385−392.
(22) Mouille, G.; Robin, S.; Lecomte, M.; Pagant, S.; Hofte, H. Classification and identification of Arabidopsis cell wall mutants using Fourier Transform InfraRed (FT-IR) microspectroscopy. *Plant J.* **2003**, *35*, 393−404.
(23) Kacurakova, M.; Capek, P.; Sasinkova, V.; Wellner, N.; Ebringerova, A. FT-IR study of plant cell wall model compounds: pectic polysaccharides and hemicelluloses. *Carbohydr. Polym.* **2000**, *43*, 195−203.
(24) Marchessault, R. H.; Liang, C. Y. The infrared spectra of crystalline polysaccharides. VIII. Xylans. *J. Polym. Sci.* **1962**, *59*, 357−378.
(25) Kacurakova, M.; Ebringerova, A.; Hirsch, J.; Hromadkova, Z. Infrared Study of Arabinoxylans. *J. Sci. Food Agric.* **1994**, *66*, 423−427.
(26) Kacurakova, M.; Wellner, N.; Ebringerova, A.; Hromadkova, Z.; Wilson, R. H.; Belton, P. S. Characterisation of xylan-type polysaccharides and associated cell wall components by FT-IR and FT-Raman spectroscopies. *Food Hydrocolloids* **1999**, *13*, 35−41.
(27) Ordaz-Ortiz, J. J.; Guillon, F.; Tranquet, O.; Dervilly-Pinel, G.; Tran, V.; Saulnier, L. Specificity of monoclonal antibodies generated against arabinoxylans of cereal grains. *Carbohydr. Polym.* **2004**, *57*, 425−433.
(28) Guillon, F.; Tranquet, O.; Quillien, L.; Utille, J.-P.; Ordaz Ortiz, J. J.; Saulnier, L. Generation of polyclonal and monoclonal antibodies against arabinoxylans and their use for immunocytochemical location of arabinoxylans in cell walls of endosperm of wheat. *J. Cereal Sci.* **2004**, *40*, 167−182.
(29) Jollife, I. T. *Principal Component Analysis*; Springer-Verlag: New York, 1986.
(30) Cael, J. J.; Koenig, J. L.; Blackwell, J. Infrared and Raman spectroscopy of carbohydrates. *Carbohydr. Res.* **1973**, *29*, 123−134.
(31) Van Soest, J. J. G.; de Wit, D.; Tournois, H. Retrogradation of potato starch as studied by Fourier transform infrared spectroscopy. *Starch/Staerke* **1994**, *46*, 453−457.
(32) Van Soest, J. J. G.; Tournois, H.; de Wit, D.; Vliegenthart, J. F. G. Short-range structure in (partially) crystalline potato starch determined with attenuated total reflectance Fourier transform IR spectroscopy. *Carbohydr. Res.* **1995**, *279*, 201−214.
(33) Barron, C.; Parker, M. L.; Mills, E. N. C.; Rouau, X.; Wilson, R. H. FTIR imaging of wheat endosperm cell walls in situ reveals compositional and architectural heterogeneity related to grain hardness. *Planta* **2005**, *220*, 667−677.
(34) Mills, E. N. C.; Parker, M. L.; Wellner, N.; Toole, G.; Feeney, K.; Shewry, P. R. Chemical imaging: the distribution of ions and molecules in developing and mature wheat grain. *J. Cereal Sci.* **2005**, *41*, 193−201.
(35) Yu, P. Molecular chemistry imaging to reveal structural features of various plant feed tissues. *J. Struct. Biol.* **2005**, *150*, 81−89.

Received for review May 18, 2005. Revised manuscript received July 7, 2005. Accepted July 7, 2005. We thank ULICE and Arvalis for their financial support.

JF051145Y